THE JOURNAL OF PHYSICAL CHEMISTRY Letters

Letter

pubs.acs.org/JPCL

Toward Highlighting the Ultrafast Electron Transfer Dynamics at the Optically Dark Sites of Photocatalysts

Sophie E. Canton,*[,†] Xiaoyi Zhang,*[,‡] Jianxin Zhang,[§] Tim B. van Driel,[∥] Kasper S. Kjaer,[⊥] Kristoffer Haldrup,[∥] Pavel Chabera,[#] Tobias Harlang,[#] Karina Suarez-Alcantara,[†] Yizhu Liu,[§] Jorge Pérez,[§] Amélie Bordage,[○,▽] Mátyás Pápai,[○] György Vankó,[○] Guy Jennings,[‡] Charles A. Kurtz,[‡] Mauro Rovezzi,[◆] Pieter Glatzel,[◆] Grigory Smolentsev,[#] Jens Uhlig,[#] Asmus O. Dohn,[¶] Morten Christensen,[∥] Andreas Galler,[●] Wojciech Gawelda,[●] Christian Bressler,[●] Henrik T. Lemke,[◇] Klaus B. Møller,[⊥] Martin M. Nielsen,[∥] Reiner Lomoth,[□] Kenneth Wärnmark,[§] and Villy Sundström*[,#]

[†]Department of Synchrotron Radiation Instrumentation, P.O. Box 118, Lund University, 22100 Lund, Sweden

[‡]X-ray Sciences Division, Argonne National Laboratory, 9700 South Cass Avenue, Argonne, Illinois 60439, United States

[§]Centre for Analysis and Synthesis, Department of Chemistry, Lund University, S-22100 Lund, Sweden

[∥]Centre for Molecular Movies, Department of Physics, Technical University of Denmark, DK-2800, Lyngby, Denmark

[⊥]Centre for Molecular Movies, Niels Bohr Institute, University of Copenhagen, DK-2100, Copenhagen, Denmark

[#]Chemical Physics Department, P.O. Box 118, Lund University, S-22100 Lund, Sweden

[○]Wigner Research Centre for Physics, Hungarian Academy Sciences, H-1525 Budapest, P.O.B. 49, Hungary

[▽]Institut Néel, CNRS et Université Joseph Fourier, BP 166, F-38042 Grenoble Cedex 9, France

[◆]European Synchrotron Radiation Facility, BP 220, F-38043 Grenoble, France

[¶]Department of Chemistry, Technical University of Denmark, DK-2800, Kgs. Lyngby, Denmark

[●]European XFEL Facility, Albert-Einstein Ring 19, D-22 761 Hamburg, Germany

[◇]SLAC National l Accelerator Laboratory, Linac Coherent Light Source, Menlo Park, California 94025, United States

[□]Department of Chemistry-Ångström Laboratory, Box 523, Uppsala University, S-75120 Uppsala, Sweden

Supporting Information

ABSTRACT: Building a detailed understanding of the structure−function relationship is a crucial step in the optimization of molecular photocatalysts employed in water splitting schemes. The optically dark nature of their active sites usually prevents a complete mapping of the photoinduced dynamics. In this work, transient X-ray absorption spectroscopy highlights the electronic and geometric changes that affect such a center in a bimetallic model complex. Upon selective excitation of the ruthenium chromophore, the cobalt moiety is reduced through intramolecular electron transfer and undergoes a spin flip accompanied by an average bond elongation of 0.20 ± 0.03 Å. The analysis is supported by simulations based on density functional theory structures (B3LYP*/TZVP) and FEFF 9.0 multiple scattering calculations. More generally, these results exemplify the large potential of the technique for tracking elusive intermediates that impart unique functionalities in photochemical devices.

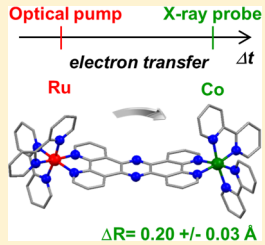

SECTION: Spectroscopy, Photochemistry, and Excited States

Harnessing efficient water splitting is a conceptual and technical milestone in the development of carbon-neutral fuel sources that has yet to be reached.[1,2] This chemical reaction presents high thermodynamic and kinetic barriers associated with bond breaking and formation, as it requires the coupled evolution of oxygen and hydrogen.[3,4] Among the various strategies that employ solar energy, homogeneous photocatalysis offers distinct prospects for selectivity and tunability. Motivated by early examples of water reduction cascades inspired by the Z-scheme of natural photosynthesis,[5] the exploration of the so-called molecular approach to hydrogen generation[6,7] has since then been continuously pursued.[8−12] In the three-component system[13−15] depicted in Figure 1a, the photosensitizer (PS) absorbs a fraction of the incident light. The energy is used to transfer electrons from the sacrificial donor (SD) to the relay (R) that reduces the catalytic center (C). Once two electrons have been accumulated, this last species further reacts with aqueous protons (H^+) to produce hydrogen (H_2). In the targeted solar fuel systems, water itself will eventually be the source of electrons. The general applicability of the cycle is evidenced by the growing

Received: May 16, 2013
Accepted: May 23, 2013
Published: May 23, 2013

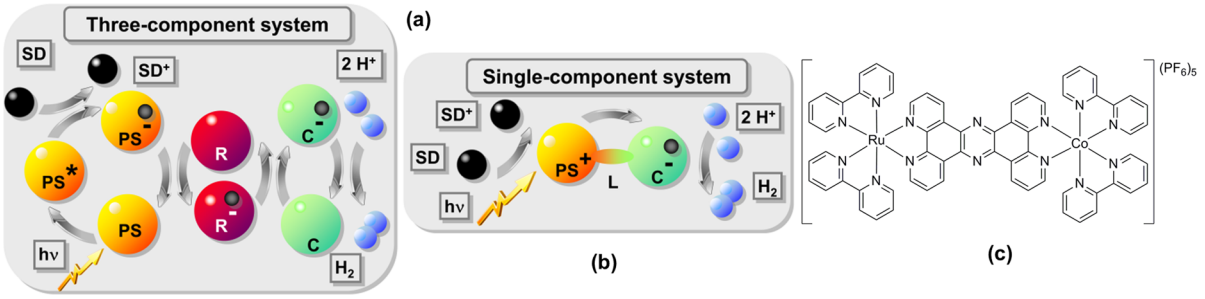

Figure 1. (a) Schematic of a three-component system, comprising a photosensitizer (PS), a sacrifical donor (SD), a relay (R) and a catalytic center (C). The intermediate species formed during the cycle are also indicated, see text. (b) Schematic of a one-component complex integrating these constituents. (c) Molecular structure of the model complex $[(bpy)_2Ru^{II}(tpphz)^1Co^{III}(bpy)_2](PF_6)_5$.

variety of components that have been combined successfully, with particular focus on incorporating inexpensive, abundant and nontoxic first-row elements.[16−20] Although such flexibility should provide ample latitude for optimization, determining the causes for limited performances *in-operando* (e.g., low turnover rates or degradation)[21,22] is often difficult. A promising route, suggested by the structural organization found within photosynthetic organisms, merges the basic constituents of a three-component system into a single photochemical molecular device (Figure 1b).[23,24] The conjugated linker (L) that connects the light-harvesting and the redox active moieties alleviates the participation of diffusion. This bridge can also act as electron relay and reservoir[25,26] when it mediates directional charge transfer via its acceptor orbitals. Studies resorting to ultrafast optical spectroscopies in the UV−visible region have established definite correlations between the overall efficiency, the molecular architecture, and the deactivation pathways from the initial Franck−Condon point to the manifold of low-lying excited states located on the bridge.[27,28] However, these techniques probe optical transitions between delocalized orbitals so that they are usually insensitive to dipole-forbidden channels and bear the signatures of atomic rearrangements only indirectly. Consequently, a comprehensive understanding of the structure−function relationship at the catalytic center remains to be obtained for this important class of complexes. The present work demonstrates how ultrafast transient X-ray absorption (XA) spectroscopy[29,30] can be added to the analytical toolbox available to characterize the photoinduced dynamics that take place at optically dark active centers.

The complex $[(bpy)_2Ru^{II}(tpphz)^1Co^{III}(bpy)_2](PF_6)_5$ (Figure 1c), where bpy = 2,2′- bipyridine, tpphz = tetrapyrido (3,2-*a*:2′3′-*c*:3″,2″-*h*::2‴,3‴-*j*) phenazine,[31] represents a prototypical model for intramolecular precatalysts employed in light-driven hydrogen evolution. An improved protocol for its synthesis from the building block $[(bpy)_2Ru^{II}(tpphz)](PF_6)_2$ is given in SI1. Employing $[Co^{III}(bpy)_2(OTf)_2]OTf$ instead of $[Co^{III}(bpy)_2Cl_2]Cl$ produced the analytically pure bimetallic compound in 75% yield as compared to 16%.[31] The steady-state optical absorption and emission spectra are shown in Figure 2a for $[(bpy)_2Ru^{II}(tpphz)]^{2+}$ and $[(bpy)_2Ru^{II}(tpphz)^1Co^{III}(bpy)_2]^{5+}$ in acetonitrile (CH_3CN). These species are designated by $[Ru^{II}{=}]$ and $[Ru^{II}{=}{}^1Co^{III}]$ hereafter. The regions between 340−380 nm, 400−440 nm and 440−550 nm are assigned respectively to tpphz ligand-centered (LC), singlet metal-to-ligand charge transfer (MLCT) Ru→bpy and Ru→ $tpphz_{phen}$[32] transitions. The pronounced emission from ^{3}MLCT ($Ru\text{-}tpphz_{phen}$) is centered around 627 nm.[33] Upon coordination of the $^1Co^{III}(bpy)_2$ moiety, the absorbance

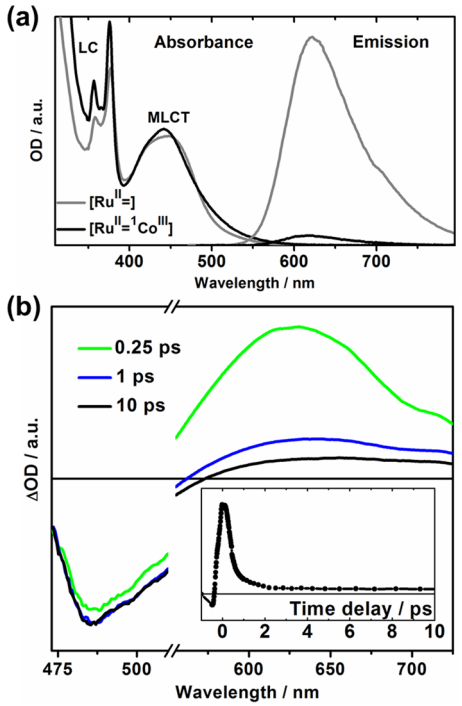

Figure 2. (a) UV−vis absorption and emission spectra for $[Ru^{II}{=}]$ and $[Ru^{II}{=}{}^1Co^{III}]$ in CH_3CN. (b) Transient absorption spectra for $[Ru^{II}{=}{}^1Co^{III}]$ in CH_3CN at 0.2 ps, 1 ps, 10 ps after photoexcitation at 527 nm (~80 fs pulse duration). The inset shows the transient kinetics recorded at 580 nm.

is slightly modified due to the interaction at the distal bpy of tpphz. Moreover, 95% of the emission is quenched (Figure 2b). Since the $[Ru^{II}{=}]$ emission and the $[Ru^{II}{=}{}^1Co^{III}]$ absorption do not overlap significantly, Förster energy transfer can be ruled out. Cyclic voltammetry indicates that electron transfer from Ru^{II} to $^1Co^{III}$ is thermodynamically possible (SI2 in the Supporting Information). Transient absorption spectroscopy (Figure 2b and SI3) is used to determine the dynamics of the process. A broad band with a maximum at 625 nm appears quasi-instantaneously following femtosecond laser excitation at 527 nm. This is the known signature of reduced pyrazine[34,35] in dyads linked through tpphz. The kinetics at the isosbestic point between $[Ru^{II}{=}{}^1Co^{III}]$ and $[Ru^{III}{=}{}^1Co^{III}]$ obtained from spectroelectrochemistry (at 580 nm, see SI2) track any optically bright intermediate formed in the course of the charge separation. This signal largely decays within a few picoseconds, which is much faster than the few tens to hundreds of picoseconds reported for related complexes.[34,35] While the

dx.doi.org/10.1021/jz401016h | *J. Phys. Chem. Lett.* 2013, 4, 1972−1976

deactivation of the excited states is captured in the visible range, no information about the dynamics at the reduced Co center can be inferred.

By contrast, transient XA spectra acquired at the Co K edge (7709 eV) reveal both the change of oxidation state and the alterations in the local bonding environment of this optically dark site. The experimental details are given in SI4. Figure 3a displays the normalized XA coefficient μ taken without laser illumination (black) and 3 ns after excitation at 527 nm (red). The signal $\Delta\mu$ = [μ (laser on) − μ (laser off)] is shown in Figure 3b. In order to assist the analysis, it is first compared to a reference trace (Figure 3b), which is constructed by forming the difference between the steady-state XA spectra of the mononuclear complexes $[^4Co^{II}(bpy)_3]$ $(\pi t_{2g})^5(\sigma e_g)^2$ (high spin, HS) and $[^1Co^{III}(bpy)_3]$ $(\pi t_{2g})^6$ (low spin, LS) obtained under identical experimental conditions (i.e., solvent, concentration, counterion, jet speed and beamline settings). The inset contains the k^2-weighted traces, where k is the photoelectron wavevector. The similarities demonstrate positively that electron transfer is accompanied by a spin flip[36] in the relaxed photoproduct. Scaling the measurement to the reference readily delivers the excited state fraction (65 ±3%).

The transient XA fingerprints reflect the change in electronic configuration from $(\pi t_{2g})^6$ to $(\pi t_{2g})^5(\sigma e_g)^2$ and the driven atomic rearrangements. They can be explained within a simple molecular orbital description of the X-ray induced transitions. For quasi-octahedral d^6 complexes, the pre-edge feature P is attributed to the electric-quadrupole 1s → 3d transition. It corresponds to a single 1s → e_g in $^1Co^{III}$ (LS), while it splits into several unresolved multiplets for 1s → t_{2g} and 1s → e_g in $^4Co^{II}$ (HS). The available S/N ratio prevented further deconvolution. Across the near-edge region, the spectral distribution maps the unoccupied p-density of states (p-DOS). The shoulder A and the sharp white line B are ascribed to the electric-dipole promotion of a core electron to Co(4p)−N(2p) hybridized states. The population of the antibonding e_g in the Co^{II} moiety causes the Co−N bond length to increase. Consequently, the overlap between metal and ligand orbitals decreases, and the hybridized states contain less ligand contribution. The resulting stabilization accounts for a more intense 1s → 4p transition that is down shifted by about ∼1.5 eV (feature B′). FEFF 9.0 simulations of the XANES and EXAFS profiles based on structures obtained from crystallography (CS) and B3LYP*/TZVP (SI5) density functional theory (DFT) for $[^1Co^{III}(bpy)_3]$ (LS) and $[^4Co^{II}(bpy)_3]$ (HS) support the interpretation (Figure 3c). The unoccupied p-DOS at the Co and N atoms are also shown in Figure 3d,e. Since the broad features D and D′ can be traced back to single scattering of the outgoing photoelectron by the nearest-neighbor N shell, their positions approximately obey Natoli's rule,[37] $\Delta E \times R_{av}^2$ = constant, where ΔE is the photon energy above threshold. Assigning C and C′ is more intricate, as they arise from multiple scattering. Fitting the transient XA spectrum in the energy range that contains the structural information returns an average bond elongation of ΔR_{av} = 0.20 ± 0.03 Å (black curve in Figure 3b, and SI6). This value is in agreement with the known average Co−N bond lengths of 1.934 ± 0.005 Å and 2.122 ± 0.003 Å for $[^1Co^{III}(bpy)_3]$ (LS) and $[^4Co^{II}(bpy)_3]$ (HS), respectively.[38−40] The reconstructed excited state spectrum is given in SI7. Figure 4 displays the X-ray kinetics recorded at 7720 eV (A′) as a function of pump−probe delay. The inset zooms on the early times.

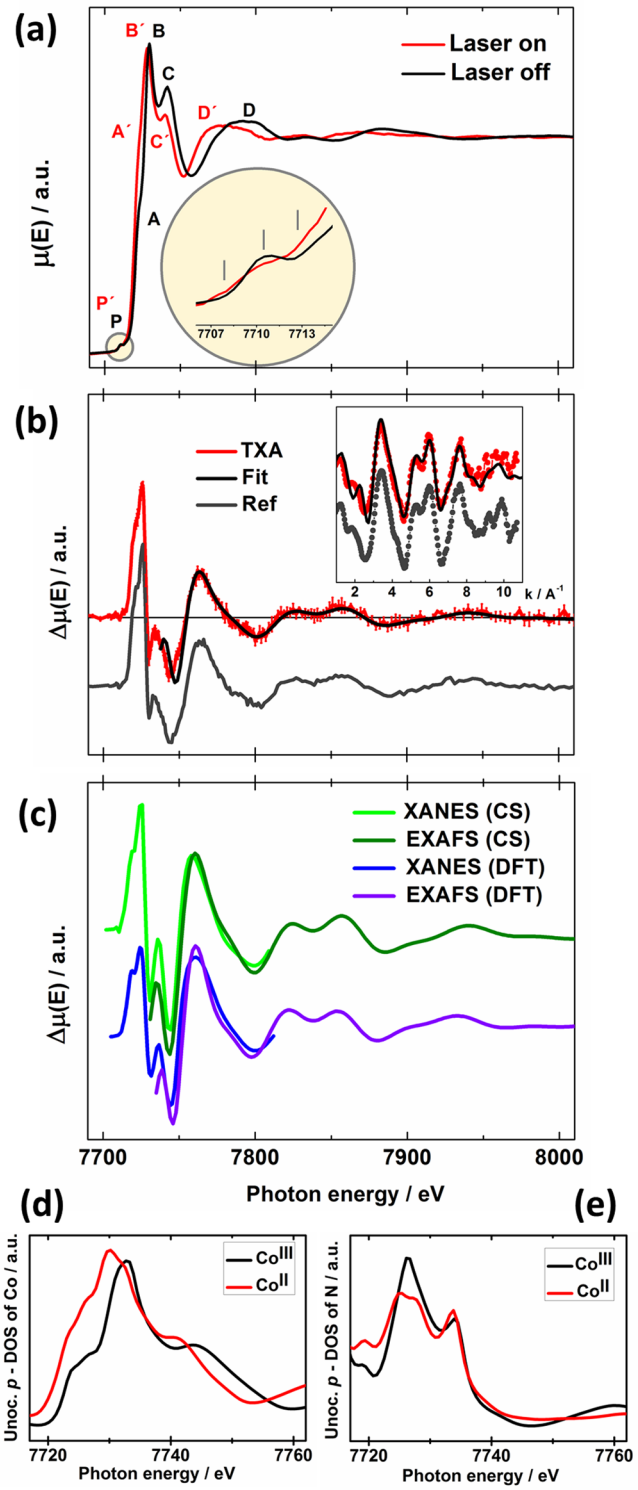

Figure 3. (a) Transient XA spectra acquired for $[Ru^{II}{=}{}^1Co^{III}]$ in CH_3CN at the Co K edge, laser off (black), and laser on (red) with a delay of 3 ns. (b) Difference spectrum [μ(laser on) − μ(laser off)], and reference spectrum. (inset) k^2-weighted traces as a function of k, the photoelectron wavevector (c) XANES and EXAFS profiles obtained from FEFF 9.0 simulations based on crystal structures (light and dark green) and DFT results (blue and violet). (d) Unoccupied p-DOS at the Co center for $[^1Co^{III}(bpy)_3]$ and $[^4Co^{II}(bpy)_3]$ obtained from FEFF 9.0 calculations based on the DFT structures. (e) Similarly, unoccupied p-DOS at the N atoms.

dx.doi.org/10.1021/jz401016h | J. Phys. Chem. Lett. 2013, 4, 1972−1976

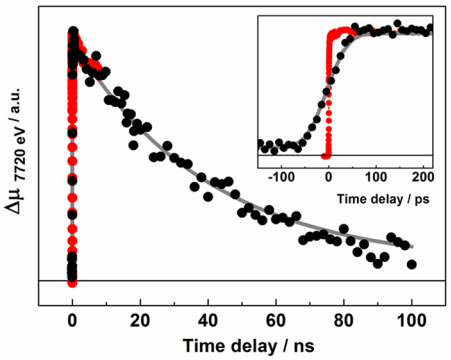

Figure 4. X-ray kinetics taken at 7720 eV (feature A′) (black) and single-exponential fit (gray). The onset of the ground state bleach recovery from transient optical kinetics measured at 490 nm is inverted and scaled for comparison (red).

With a temporal resolution limited to 80 ps, typical for synchrotron experiments, $^4Co^{II}$ (HS) appears promptly. This population decays through thermal back electron transfer with a single time constant fitted to 45 ± 2 ns (SI8). This value matches the ground state bleach recovery observed in optical transient absorption spectroscopy.[31]

To summarize, the present work illustrates how transient XA spectroscopy can *directly* monitor the coupled electronic and structural dynamics at the optically dark center of a model complex. Upon selective excitation of the ruthenium chromophore, the cobalt moiety is reduced through intramolecular electron transfer. It concurrently undergoes a spin flip accompanied by an average Co−N bond elongation of 0.20 ± 0.03 Å. The mechanisms at play on the subpicosecond time scale are still beyond the temporal resolution attainable at storage rings, but will be accessible at the X-ray free electron laser facilities that are coming online worldwide. In particular, it should be possible to detect the participation of $^2Co^{II}$ (LS), which has often been proposed as an intermediate step to rationalize ultrafast intramolecular electron transfer involving $^1Co^{III}$ (LS)/$^4Co^{II}$ (HS), but seldom identified unambiguously.[41] More generally, transient XA spectroscopy is likely to provide novel structural guidelines to refine the frontier-orbital engineering of molecular photocatalysts. So far, the main effort has been directed toward benchmarking how the peripheral substituents can induce LUMO localization on the bridge for a given architecture, a property that in turn favors high efficiency. Owing to its element-specificity and its intrinsic sensitivity to the coupling between electronic and geometric degrees of freedom, the technique may contribute to uncover the various factors that instead could promote rapid LUMO localization on the catalytic center itself, rendering the photochemical molecular device more robust toward multiple reductions. In combination with time-resolved X-ray scattering,[42,43] it should also deliver unique diagnostics about the dynamical evolution of the chemical bonds that are essential to activity and stability, e.g. halogen elimination or ligand dissociation.[44,45] Finally, the methodology will be generally applicable to a wide range of phototriggered intramolecular phenomena, where short-lived intermediates that cannot be detected optically, are the species imparting advanced functionality.

■ ASSOCIATED CONTENT

Supporting Information

SI_1: Synthesis of $[(bpy)_2Ru^{II}(tpphz)^1Co^{III}(bpy)_2](PF_6)_5$. SI_2: Cyclic voltammetry and spectroelectrochemistry. SI_3: Time-resolved optical spectroscopy. SI_4: Time-resolved X-ray absorption (XA) spectroscopy set up at 11-ID-D of the Advanced Photon Source (APS). SI_5: Computational details and results for the DFT calculations on $[^1Co^{III}(bpy)_3]$ (LS) and $[^4Co^{II}(bpy)_3]$ (HS). SI_6: Procedure for fitting the difference XA spectrum. SI_7: Reconstructed XA spectrum of the transient photoexcited state. SI_8: Fitting of the X-ray kinetics recorded at 7720 eV. This material is available free of charge via the Internet at http://pubs.acs.org.

■ AUTHOR INFORMATION

Corresponding Author

*E-mail: Sophie.Canton@maxlab.lu.se (S.E.C.); xyzhang@aps.anl.gov (X.Z.); Villy.Sundstrom@chemphys.lu.se (V.S.).

Notes

The authors declare no competing financial interest.

■ ACKNOWLEDGMENTS

This project was supported by the Swedish Research Council (SEC, VS), the Crafoord Foundation (SEC, KSA), the Science Faculty at Lund University (MAX IV and ESS initiative grant, KW, VS), the European Research Council via contracts ERC-AdvG-VISCHEM-226136 to VS and ERC-StG-259709 to GV, and the Centre for Molecular Movies through the Danish National Research Foundation and DANSCATT. G.V. acknowledges support from the Bolyai János Fellowship of the Hungarian Academy of Sciences. X.Z., G.J., C.A.K. and the use of the Advanced Photon Source, an Office of Science User Facility operated for DOE Office of Science by Argonne National Laboratory, were supported by the U.S. DOE under Contract No. DE-AC02-06CH11357. Contributions from Dr C. J. Wallentin to early synthesis work are gratefully acknowledged. We thank Pr. L. X. Chen and her group for providing the Nd:YLF regenerative amplifier laser.

■ REFERENCES

(1) Armaroli, N.; Balzani, V. The Future of Energy Supply: Challenges and Opportunities. *Angew. Chem., Int. Ed.* **2007**, *46*, 52−66.
(2) Lewis, N. S.; Nocera, D. G. Powering the Planet: Chemical Challenges in Solar Energy Utilization. *Proc. Natl. Acad. Sci.U.S.A.* **2006**, *103*, 15729−15735.
(3) Adar, E.; Degani, Y.; Goren, Z.; Willner, I. Photosensitized Electron-Transfer Reactions in β-Cyclodextrin Aqueous-Media: Effects on Dissociation of Ground-State Complexes, Charge Separation, and H_2 Evolution. *J. Am. Chem. Soc.* **1986**, *108*, 4996−4700.
(4) DeLaive, P. J.; Sullivan, B. P.; Meyer, T.; Whitten, D. G. Applications of Light-Induced Electron-Transfer Reactions - Coupling of Hydrogen Generation with Photo-Reduction of Ruthenium(II) Complexes by Triethylamine. *J. Am. Chem. Soc.* **1979**, *101*, 4007−4008.
(5) Hill, R.; Rich, P. R. A Physical Interpretation for the Natural Photosynthetic Process. *Proc. Natl. Acad. Sci. U.S.A.* **1983**, *80*, 978−982.
(6) Lehn, J. M.; Sauvage, J. P. Chemical Storage of Light Energy - Catalytic Generation of Hydrogen by Visible-Light or Sunlight - Irradiation of Neutral Aqueous-Solutions. *Nouv. J. Chim.* **1977**, *1*, 449−451.
(7) Kirch, M.; Lehn, J. M.; Sauvage, J. P. Hydrogen Generation by Visible-Light Irradiation of Aqueous-Solutions of Metal-Complexes -

Approach to the Photo-Chemical Conversion and Storage of Solar-Energy. *Helv. Chim. Acta* **1979**, *62*, 1345−1384.
(8) Heyduk, A. F.; Nocera, D. G. Hydrogen Produced from Hydrohalic Acid Solutions by a Two-Electron Mixed-Valence Photocatalyst. *Science* **2001**, *293*, 1639−1644.
(9) Esswein, A. J.; Veige, A. S.; Nocera, D. G. A Photocycle for Hydrogen Production from Two-Electron Mixed-Valence Complexes. *J. Am. Chem. Soc.* **2005**, *127*, 16641−16651.
(10) Ozawa, H.; Haga, M. A.; Sakai, K. A Photo-Hydrogen-Evolving Molecular Device Driving Visible-Light-Induced EDTA-Reduction of Water into Molecular Hydrogen. *J. Am. Chem. Soc.* **2006**, *128*, 4926−4927.
(11) Kobayashi, M.; Masaoka, S.; Sakai, K. Photoinduced Hydrogen Evolution from Water by a Simple Platinum(II) Terpyridine Derivative: A Z-Scheme Photosynthesis. *Angew. Chem., Int. Ed.* **2012**, *51*, 7431−7434.
(12) Esswein, A. J.; Nocera, D. G. Hydrogen Production by Molecular Photocatalysis. *Chem. Rev.* **2007**, *107*, 4022−4047.
(13) Kalyanasundaram, K.; Kiwi, J.; Grätzel, M. Hydrogen Evolution from Water by Visible-Light, a Homogeneous 3 Component Test System for Redox Catalysis. *Helv. Chim. Acta* **1978**, *61*, 2720−2730.
(14) Brown, G. M.; Brunschwig, B. S.; Creutz, C.; Endicott, J. F.; Sutin, N. Homogeneous Catalysis of the Photo-Reduction of Water by Visible-Light - Mediation by a tris(2,2′-bipyridine)Ruthenium(II)−Cobalt(II) Macrocycle System. *J. Am. Chem. Soc.* **1979**, *101*, 1298−1300.
(15) Crutchley, R. J.; Lever, A. B. P. Ruthenium(II) tris(bipyrazyl) Dication - A New Photocatalyst. *J. Am. Chem. Soc.* **1980**, *102*, 7128−7129.
(16) Dempsey, J. L.; Winkler, J. R.; Gray, H. B. Mechanism of H_2 Evolution from a Photogenerated Hydridocobaloxime. *J. Am. Chem. Soc.* **2010**, *132*, 16774−16776.
(17) Kluwer, A. M.; Kapre, R.; Hartl, F.; Lutz, M.; Spek, A. L.; Brouwer, A. M.; van Leeuwen, P. W. N. M.; Reek, J. N. H. Self-Assembled Biomimetic [2Fe2S]-Hydrogenase-Based Photocatalyst for Molecular Hydrogen Evolution. *Proc. Natl. Acad. Sci.* **2009**, *106*, 10460−10465.
(18) Losse, S.; Vos, J. G.; Rau, S. Catalytic Hydrogen Production at Cobalt Centres. *Coord. Chem. Rev.* **2010**, *254*, 2492−2504.
(19) Lazarides, T.; McCormick, T.; Du, P.; Luo, G.; Lindley, B.; Eisenberg, R. Making Hydrogen from Water Using a Homogeneous System without Noble Metals. *J. Am. Chem. Soc.* **2009**, *131*, 9192−9193.
(20) Fihri, A.; Artero, V.; Razavet, M.; Baffert, C.; Leibl, W.; Fontecave, M. Cobaloxime-Based Photocatalytic Devices for Hydrogen Production. *Angew. Chem., Int. Ed.* **2008**, *47*, 564−567.
(21) Tinkler, L. L.; McDaniel, N. D.; Bernhard, S. Progress Towards Solar-Powered Homogeneous Water Photolysis. *J. Mater. Chem.* **2009**, *19*, 3328−3337.
(22) Goldsmith, J. I.; Hudson, W. R.; Lowry, M. S.; Anderson, T. H.; Bernhard, S. Discovery and High-Throughput Screening of Heteroleptic Iridium Complexes for Photoinduced Hydrogen Production. *J. Am. Chem. Soc.* **2005**, *127*, 7502−7510.
(23) Rau, S.; Walther, D.; Vos, J. G. Inspired by Nature: Light Driven Organometallic Catalysis by Heterooligonuclear Ru(II) Complexes. *Dalton Trans.* **2007**, 915−919.
(24) Inagaki, A.; Akita, M. Visible-Light Promoted Bimetallic Catalysis. *Coord. Chem. Rev.* **2010**, *254*, 1220−1239.
(25) Rau, S.; Schaefer, B.; Gleich, D.; Anders, E.; Rudolph, M.; Friedrich, M.; Goerls, H.; Henry, W.; Vos, J. G. A Supramolecular Photocatalyst for the Production of Hydrogen and the Selective Hydrogenation of Tolane. *Angew. Chem., Int. Ed.* **2006**, *45*, 6215−6218.
(26) Elvington, M.; Brown, J.; Arachchige, S. M.; Brewer, K. J. Photocatalytic Hydrogen Production from Water Employing a Ru, Rh, Ru Molecular Device for Photoinitiated Electron Collection. *J. Am. Chem. Soc.* **2007**, *129*, 10644−10645.
(27) Tschierlei, S.; Karnahl, M.; Presselt, M.; Dietzek, B.; Guthmuller, J.; Gonzalez, L.; Schmitt, M.; Rau, S.; Popp, J. Photochemical Fate: The First Step Determines Efficiency of H_2 Formation with a Supramolecular Photocatalyst. *Angew. Chem., Int. Ed.* **2010**, *49*, 3981−3984.
(28) Nitadori, H.; Takahashi, T.; Inagaki, A.; Akita, M. Enhanced Photocatalytic Activity of α-Methylstyrene Oligomerization through Effective Metal-to-Ligand Charge-Transfer Localization on the Bridging Ligand. *Inorg. Chem.* **2012**, *51*, 51−62.
(29) Chen, L. X.; Jager, W. J. H.; Jennings, G.; Gosztola, D. J.; Munkholm, A.; Hessler, J. P. Capturing a Photoexcited Molecular Structure through Time-Domain X-ray Absorption Fine Structure. *Science* **2001**, *292*, 262−264.
(30) Bressler, Ch.; Milne, C.; Pham, V. -T.; ElNahhas, A.; van der Veen, R. M.; Gawelda, W.; Johnson, S.; Beaud, P.; Grolimund, D. Kaiser et al. Femtosecond XANES Study of the Light-Induced Spin Crossover Dynamics in an Iron(II) Complex. *Science* **2009**, *323*, 489−492.
(31) Toreida, H.; Nozaki, K.; Yoshimura, A.; Ohno, T. Low Quantum Yields of Relaxed Electron Transfer Products of Moderately Coupled Ruthenium(II)−Cobalt(III) Compounds on the Subpicosecond Laser Excitation. *J. Phys. Chem. A* **2004**, *108*, 4819−4829.
(32) Bolger, J.; Gourdon, A.; Ishow, H.; Launay, J.-P. Mononuclear and Binuclear Tetrapyrido[3,2-α:2′,3′-c:3″,2‴-h:2‴,3‴-j]phenazine (tpphz) Ruthenium and Osmium Complexes. *Inorg. Chem.* **1996**, *35*, 2937−2944.
(33) Flamigni, L.; Encinas, S.; Barigelletti, F.; MacDonnell, F. M.; Kim, K. J.; Puntoriero, F.; Campagna, S. Excited-State Interconversion between Emissive MLCT Levels in a Dinuclear Ru(II) Complex Containing a Bridging Ligand with an Extended π System. *Chem. Commun.* **2000**, 1185−1186.
(34) Chiorboli, C.; Rodgers, M. A. J.; Scandola, F. Ultrafast Processes in Bimetallic Dyads with Extended Aromatic Bridges. Energy and Electron Transfer Pathways in Tetrapyridophenazine-Bridged Complexes. *J. Am. Chem. Soc.* **2003**, *125*, 483−491.
(35) Tschierlei, S.; Presselt, M.; Kuhnt, C.; Yartsev, A.; Pascher, T.; Sundstrom, V.; Karnahl, M.; Schwalbe, M.; Schaefer, B.; Rau.; et al. Photophysics of an Intramolecular Hydrogen-Evolving Ru−Pd Photocatalyst. *J. Chem. Eur. J.* **2009**, *15*, 7678−7688.
(36) Krivokapic, I.; Zerara, M.; Daku, M. L.; Vargas, A.; Enachescu, C.; Ambrus, C.; Tregenna-Piggott, P.; Amstutz, N.; Krausz, E.; Hauser, A. Spin-Crossover in Cobalt(II) Imine Complexes. *Coord. Chem. Rev.* **2007**, *251*, 364−378.
(37) Natoli, C. R. Near Edge Structure III. *Springer Proc. Phys.* **1984**, *2*, 38−42.
(38) Liu, W.; Xu, W.; Lin, J.-L.; Xie, H.-Z. Tris(2,2′-bipyridine-κ(2)N:N′)Cobalt(III) Trichloride Tetrahydrate. *Acta Crystallogr.* **2008**, *E64*, M1586−U987.
(39) Du, M.; Zhao, X.-J.; Cai, H. Crystal Structure of tris(2,2′-bipyridine)Cobalt(III) Triperchlorate Dihydrate, $[Co(C_{10}H_8N_2)_3](ClO_4)_3{\cdot}2H_2O$. *Z. Kristallogr. NCS* **2004**, *219*, 463−465.
(40) Sieber, R.; Decurtins, S.; Stoeckli-Evans, H.; Wilson, C.; Yufit, D.; Howard, J. A. K.; Capelli, S. C.; Hauser, A. A Thermal Spin Transition in $[Co(bpy)_3][LiCr(ox)_3]$ (ox = $C_2O_4^{2-}$; bpy = 2,2′-bipyridine). *Chem.—Eur. J.* **2000**, *6*, 361−368.
(41) Turner, J. W.; Schultz, F. A. Coupled Electron-Transfer and Spin-Exchange Reactions. *Coord. Chem. Rev.* **2001**, *219*, 81−97.
(42) Christensen, M.; Haldrup, K.; Bechgaard, K.; Feidenhans'l, R.; Kong, Q.; Cammarata, M.; Lo Russo, M.; Wulff, M.; Harrit, N.; Nielsen, M. M. Time-Resolved X-ray Scattering of an Electronically Excited State in Solution. Structure of the $^3A_{2u}$ State of Tetrakis-μ-pyrophosphitodiplatinate(II). *J. Am. Chem. Soc.* **2009**, *131*, 502−508.
(43) Ihee, H.; Wulff, M.; Kim, J.; Adachi, S. Ultrafast X-ray Scattering: Structural Dynamics from Diatomic to Protein molecules. *Int. Rev. Phys. Chem.* **2010**, *29*, 453−520.
(44) Cook, T. R.; Surendranath, Y.; Nocera, D. G. Chlorine Photoelimination from a Diplatinum Core: Circumventing the Back Reaction. *J. Am. Chem. Soc.* **2009**, *131*, 28−29.
(45) Teets, T. S.; Cook, T. R.; McCarthy, B. D.; Nocera, D. G. Oxygen Reduction to Water Mediated by a Dirhodium Hydrido−Chloride Complex. *J. Am. Chem. Soc.* **2011**, *133*, 8114−8117.